ARTICLE NO. 77-1080

Load Factor Response of Digitally Controlled Aircraft

Dinesh A. Keskar* and Gary L. Slater†
University of Cincinnati, Cincinnati, Ohio

The effect of sampling rate on the stochastic response of a linear aircraft model and on the interaction of sampling rate selection with neglected dynamic modes in the control model is examined. Control laws are computed from optimal discrete regulator theory using both the rigid-body and flexible-body assumptions. The conclusions are that, for the aircraft under consideration, the rigid-body feedback laws are adequate to insure good system response at fast sampling rates; however, at slow sampling rates, less than about 10 samples per second, the control law based on rigid-body assumptions rapidly deteriorates, whereas the accurate control model maintains good control characteristics.

Nomenclature

A = state cost matrix
B = control cost matrix
C = coupling term in the performance index
C^* = motion variable defined in Eq. (23)
D,H,Φ_z,Γ_z = terms representing discrete notch filter, Eq. (21)
F = system matrix
G = control distribution matrix
g = acceleration due to gravity
h = altitude
I = identity matrix
J = performance index
K = control gain matrix
l_x = distance from center of gravity to the point where vertical acceleration is measured
M = Mach number
M_q,M_α,M_δ = aerodynamic moment coefficient
n_Z = normal acceleration
q = pitch rate
S = solution of matrix Riccati equation
s = Laplace transform
T = sampling interval
u = control vector
U_0 = velocity
V_{co} = crossover velocity
x = state vector
x_1 = bending mode state
Z = vertical axis (Fig. 1)
$Z_\alpha,Z_{\delta e}$ = aerodynamic force coefficients
z = state vector for discrete notch filter representation, Eq. (21)
Z_1 = bending mode deflection
Z_1' = bending mode slope
α = angle of attack
α_g = external disturbance
δ_e = elevator control input
δ_c = commanded elevator deflection
ρ = weighting on elevator control input
Φ = transition matrix
Γ_1 = discrete input distribution matrix
ω_1 = first mode frequency
ω_n = notch filter frequency
ζ = damping

Subscripts

g = at rate-gyro location
m = measured
p = at pilot station
R = due to rigid-body motion (Fig. 3)
S = due to structural motion (Fig. 3)
ss = steady state

Presented as Paper 77-1080 at the AIAA 1977 Guidance and Control Conference, Hollywood, Fla., Aug. 8-10, 1977; submitted Sept. 29, 1977; revision received Oct. 13, 1978.

Index category: Guidance and Control.

*Graduate Research Assistant, Dept. of Aerospace Engineering and Applied Mechanics. Student Member AIAA.

†Associate Professor, Dept. of Aerospace Engineering and Applied Mechanics. Member AIAA.

Introduction

DURING the last decade, industry has shown a tendency to replace analog components by digital computers. The advantages of digital computers over analog systems are greater accuracy, flexibility, and enhanced logic capability. The principal disadvantage of a digital computer in a control loop is its discrete mode of operation. The choice of sampling rate for the digital system is based on many factors, including the computer internal clock, complexity of required computations, and time response to control inputs.

Economically, the best choice is generally the slowest sample rate which allows all performance specifications to be met, as this would reduce the cost of the system and allow use of a more complex control model. However, factors such as closed-loop bandwidth, sensitivity to parameter variation, and the effect of random disturbances favor an increase in sampling rate.

Sampling rate selection for aircraft is sometimes based on a specific multiple of the highest important bending mode. Recently, Berman[1] introduced a concept that the sampling rate is independent of the bending modes and should be based on response to external disturbances. He developed an algorithm which considers system dynamics, sensor noise, and external disturbances to determine maximum permissible sampling time, the optimal state estimator, and feedback gains to yield desired response. The sample rate is determined by propagating the state covariance matrix until error bounds are exceeded. When this technique was applied to a V/STOL aircraft, it yielded a sampling frequency which was, in fact, slower than the highest bending mode frequency.

An alternate approach by Katz and Powell[2] examines forced and unforced response in several ways to determine sample rates for a model of the F-4 aircraft. Their conclusion is that sample rates on the order of 10-20 samples per second are appropriate using an optimal control law.

The effect of sampling period on optimal sampled data linear regulators was studied by Kuo,[3] who showed that the first-order sensitivity of the Riccati matrix is zero and its second-order sensitivity is the solution of a Lyapunov-type matrix equation.

Levis et al.[4] related the sampling rate to the behavior of a quadratic performance index for a class of discretely controlled, continuous systems. For the class of systems studied (simple first- and second-order systems), the effect of sampling was to increase the performance index. They concluded that for stable plants, the maximum increase in the optimal performance index caused by sampling was about 25%, while the performance index of an unstable plant increased rapidly as the sampling period increased.

In this paper, an attempt is made to examine the effect of sampling rate on several approximations commonly made in determining feedback laws for a flexible aircraft. The effect of sampling rate on the covariances of state and control are investigated for a class of linear systems with a quadratic performance index. The system equations and the performance index are continuous, but the control is discretized at a fixed sample rate. The approach taken is to discretize the system and performance index and obtain the optimal feedback gains and covariances from optimal discrete systhesis. The method is applied to the determination of stochastic response for the longitudinal control of a small attack aircraft.

Several different approaches to the determination of feedback laws are investigated and compared. The suboptimal approach is to determine a set of feedback laws, completely ignoring structural motion. If the effects of the structural motion are significant, a digital notch filter is inserted into the control loop to filter commanded control deflections to the aircraft. This suboptimal approach is compared with the optimal solutions which include the structural motions in the model. For all cases, the effect of sampling rate on the mean square response is obtained.

Optimal Discrete Regulator

A regulator is a feedback controller designed to keep a stationary system within an acceptable deviation from a reference condition while using a minimum amount of control.

The linear quadratic regulator problem can be formulated as

$$x_{i+1}=\Phi x_i+\Gamma_1 u_i \qquad (x_0 \text{ given}) \tag{1}$$

Let A and B be symmetric matrices, non-negative and positive definite, respectively.

Define the performance index as

$$J=\frac{1}{2}\left[\sum_{i=0}^{N-1} x_i^T A x_i+u_i^T B u_i\right]+\frac{1}{2}[x_N^T A x_N] \tag{2}$$

The optimal linear controller is a control law $u_i=K_i x_i$ that minimizes the performance index J. The minimum value of the performance index is[2,5]

$$J_{\min.}=\tfrac{1}{2}x_0^T S_0 x_0$$

where S_0 is the solution of the matrix Riccati difference equation in S_j:

$$S_j=\Phi^T(s_{j+1}^{-1}+\Gamma_1 B^{-1}\Gamma_1^T)^{-1}\Phi+A \quad \begin{bmatrix} j=N-1,\ldots,0 \\ S_N=A \end{bmatrix} \tag{3}$$

The steady-state regulator is defined as the control which results when $N\to\infty$, in which case S_j reaches a steady-state S_{ss} and the feedback law is stationary:

$$u_i=-B^{-1}\Gamma_1^T(\Phi^{-1})^T(s_{ss}-A)x_i \tag{4}$$

In the steady state, the matrix Riccati difference equation is reduced to a second-order matrix algebraic equation:

$$S_{ss}=\Phi^T(S_{ss}^{-1}+\Gamma_1 B^{-1}\Gamma_1^T)^{-1}\Phi+A \tag{5}$$

Numerical results for the steady-state regulator problem are obtained in this paper by solving Eq. (5) using the eigenvector decomposition method for discrete systems.[2]

Discretization Procedure

The system under consideration is a linear continuous system of the form

$$\dot{x}=Fx+Gu \tag{6}$$

with continuous performance index

$$J=\frac{1}{2}\int_0^\infty [x^T u^T]\begin{bmatrix} A & C \\ C^T & B \end{bmatrix}\begin{bmatrix} x \\ u \end{bmatrix} \mathrm{d}t \tag{7}$$

where the control is constrained to be of the form

$$u(t)=u_i \qquad iT\le t<(i+1)T \tag{8}$$

The solution of Eq. (6) is easily shown to be in the form given by Eq. (1) where

$$\Phi=\Phi(T)=e^{FT} \tag{9}$$

$$\Gamma_1=\Gamma_1(T)=\int_0^T \Phi(\tau)G\mathrm{d}\tau \tag{10}$$

The continuous cost function, Eq. (7), can be reformulated similarly as a discrete cost function:

$$J=\frac{1}{2}\sum_{i=0}^{N-1}[x_i^T \quad u_i^T]\begin{bmatrix} P & Q \\ Q^T & R \end{bmatrix}\begin{bmatrix} x_i \\ u_i \end{bmatrix} \tag{11}$$

where

$$P=\int_0^T \Phi^T(\tau)A\Phi(\tau)\mathrm{d}\tau$$

$$Q=\int_0^T [\Phi^T(\tau)A\Gamma_1(\tau)+\Phi^T(\tau)C]\mathrm{d}\tau$$

$$R=\int_0^T [\Gamma_1^T(\tau)A\Gamma_1(\tau)+B+\Gamma_1^T(\tau)C+C^T\Gamma_1(\tau)]\mathrm{d}\tau \tag{12}$$

Algorithms for the evalution of P, Q, R in Eq. (12) can be found in Ref. 2 for the case where $C=0$. In the case considered here with $C\neq 0$ and where F is nonsingular, these additional terms can be easily calculated as

$$\int_0^T \Phi^T(\tau)C\mathrm{d}\tau=\{C^T F^{-1}[\Phi-I]\}^T \tag{13a}$$

$$\int_0^T C^T\Gamma_1(\tau)\mathrm{d}\tau=C^T F^{-1}\{F^{-1}[\Phi-I]-IT\}G \tag{13b}$$

Effects of Sampling on Response

The primary goal of the controllers designed in this section is to minimize the normal acceleration at the pilot station. Several approaches to the determination of the required

sample rate are investigated. The suboptimal approach is to determine a set of feedback laws, completely ignoring the structural motion. If the structural effects are significant, a digital notch filter is inserted into the control loop to filter commanded control deflections to the aircraft. This approach is compared to the optimal model which includes the structural motion in the mathematical model. In all cases, the effect of sampling rate on the mean square response is obtained.

The vehicle used in this study is a model of a small attack aircraft. The geometry of this aircraft is shown in Fig. 1. The equations of motion based on the short-period approximation with random gusts modeled as white noise perturbations in the angle of attack are

$$\begin{bmatrix} s-M_q & -M_\alpha \\ -1 & s-Z_w \end{bmatrix} \begin{bmatrix} q \\ \alpha \end{bmatrix} = \begin{bmatrix} M_{\delta_e} \\ Z_{\delta_e} \\ \hline U_0 \end{bmatrix} \delta_e + \begin{bmatrix} M_\alpha \\ Z_w \end{bmatrix} \alpha_g \tag{14}$$

The bending mode is modeled as a second-order system driven by the elevator input and the total angle of attack ($\alpha + \alpha_g$). The bending equations are

$$(s^2 + 2\zeta_1\omega_1 s + \omega_1^2)x_1 = Z_{1\delta_e} Z_{\delta_e}\delta_e + Z_{1w}Z_\alpha\alpha + Z_{1w}Z_\alpha\alpha_g \tag{15}$$

where Z_1 is the shape of the first mode. Measurements are taken of the angle of attack and pitch rate. These measurements include both the rigid-body motion and the structural motion.

Output equations are

$$\begin{bmatrix} \alpha_m \\ q_m \end{bmatrix} = \begin{bmatrix} 0 & 1 & -Z_{1P} \\ 1 & 0 & -Z'_{1g}s \end{bmatrix} \begin{bmatrix} q \\ \alpha \\ x_1 \end{bmatrix} \tag{16}$$

Numerical examples in this paper are based on the data shown in Table 1.

Table 1 Numerical data

h	$=0$	$Z_{\delta e}$	$=-275\ \text{ft/s}^2$
M	$=0.9$	$Z_{1\delta e}$	$=-0.65$
U_0	$=100\ \text{ft/s}$	Z_{1g}	$=+0.025$
$M_{\delta e}$	$=-53\ \text{s}^{-2}$	Z_{1P}	$=-0.25$
Z_α	$=-2950\ \text{ft/s}^2$	ξ_1	$=0.01$
ω_1	$=25\ \text{rad/s}$	Z_w	$=-3.4\ \text{s}^{-1}$
Z_{1w}	$=0.2$	M_q	$=-1.34\ \text{s}^{-1}$
M_α	$=-40\ \text{s}^{-2}$		

Open loop poles

Rigid body $-2.37 \pm 6.25j$
Bending modes $-0.25 \pm 25j$

Notch filter

$\omega_n = 25\ \text{rad/s}$
$\zeta_n = 0.01$

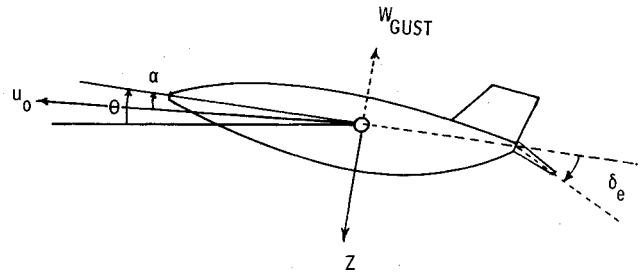

Fig. 1 Geometry of aircraft.

Rigid-Body Model

The rigid-body model of the aircraft is obtained from Eqs. (14-16) by deleting Eq. (15) and the terms relating to x_1 in Eq. (16). Using this second-order model, control laws were derived by minimization of the continuous performance index:

$$J = \frac{1}{2}\int_0^\infty (n_Z^2 + \rho\delta_e^2)\,dt \tag{17}$$

where n_Z is rigid-body normal acceleration measured at the pilot's station, given by

$$n_Z = \left(\frac{U_0}{g} + \frac{l_x}{g}s\right)q + \left(-\frac{U_0}{g}s\right)\alpha \tag{18}$$

The weighting factor ρ on the elevator deflection δ_e is chosen so as to give acceptable closed-loop eigenvalues. The root locus of optimal closed-loop poles varying ρ corresponds to the case of $V_{c0} = 0$ in Fig. 2. (Note that as $\rho \to \infty$, the optimal closed-loop poles approach the open-loop poles.)

The optimal second-order analysis is a suboptimal control for the actual dynamical system, which includes both the rigid-body and the structural motions. The suboptimal controller is analyzed and compared to an optimal controller using the model, Eqs. (14) and (15), and the same performance index as in Eq. (17) where the load factor equation is now modified to

$$n_Z = [(U_0/g) + (l_x/g)s]q - sU_0/g\alpha - (Z_{l_x}/g)s^2x_1 \tag{19}$$

The optimal and suboptimal control laws are evaluated by comparing the load-factor response for varying sample rates.

For the suboptimal laws designed and implemented assuming only rigid-body motion, the effect of inserting a digital notch filter into the control was examined. The intent of the notch filter is to remove frequency components corresponding to the structural motion so as to isolate the rigid-body motion from the structural motion. The continuous notch filter with notch frequency ω_n and damping ζ_n is represented as

$$G_n(s) = \frac{s^2 + 2\zeta_n\omega_n s + \omega_n^2}{(s+\omega_n)^2} \tag{20}$$

This was discretized using the Tustin transformation because of its relative ease of implementation. The continuous filter was prewarped to compensate for the frequency shift associated with the Tustin substitution so that the digital notch lies at the desired frequency, as shown by Slater.[6]

The discrete notch filter can be written in state-space form as

$$z_{k+1} = \Phi_z z_k + \Gamma_z\delta_{c_k}$$
$$\delta_{e_k} = Hz_k + D\delta_{c_k} \tag{21}$$

where δ_c is the commanded elevator deflection and δ_e is the output of the filter. Augmenting the filter dynamics to the aircraft equations of motions with feedback, we obtain the

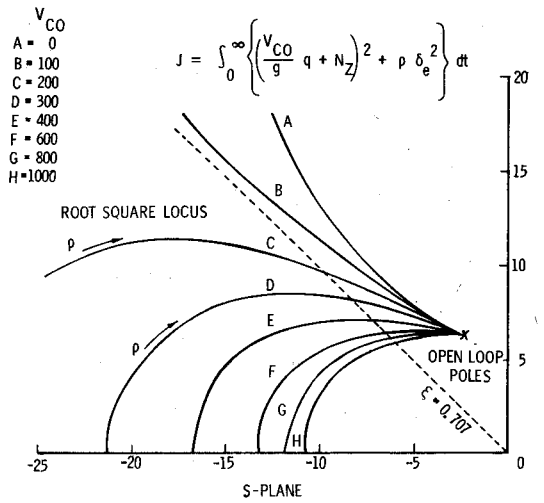

Fig. 2 Locus of roots of optimally controlled rigid-body system.

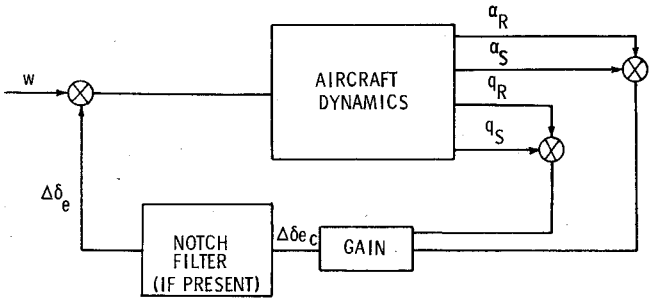

Fig. 3 Control structure for suboptimal controller.

coupled set

$$\begin{bmatrix} x \\ z \end{bmatrix}_{k+1} = \begin{bmatrix} \Phi & \Gamma_1 H \\ 0 & \Phi_z \end{bmatrix} \begin{bmatrix} x \\ z \end{bmatrix}_k + \begin{bmatrix} \Gamma_1 D \\ \Gamma_z \end{bmatrix} \delta_{c_k} + \begin{bmatrix} \Gamma_2 \\ 0 \end{bmatrix} \alpha_{g_k} \tag{22}$$

Again, the covariances of state and control can be obtained from Eq. (22) by solving the covariance equation associated with this problem using suboptimal feedback law $\delta_{c_k} = Kx_k$.

As mentioned previously, minimization of the performance index, Eq. (17), results in a system with fairly low damping ratio. To improve system damping, it was desired to put additional terms in the performance index proportional to the pitch rate. This was done by introducing the variable C^* where

$$C^* = n_Z + (V_{co}/g)q \tag{23}$$

The variable V_{co} is referred to as the crossover velocity. In this form, the C^* varible was introduced as a motion variable suitable for feedback, which tended to give good response over a wide range of dynamic pressures. Classical application of the C^* variable requires that the step response of this motion variable falls inside of a specified time-response envelope.[7] For this application, we merely use C^* as part of a linear quadratic optimization problem which minimizes the performance index

$$J = \frac{1}{2}\int_0^\infty [C^{*2} + \rho\delta_e^2]dt \tag{24}$$

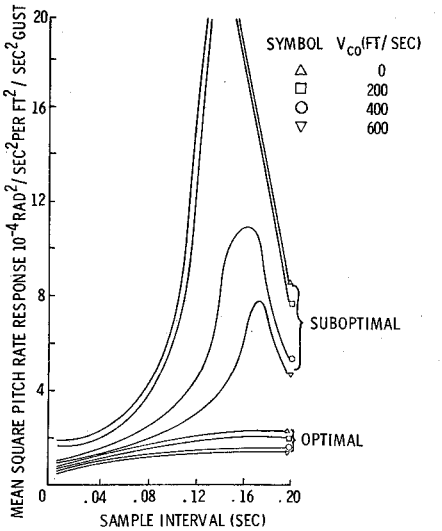

Fig. 4 Pitch rate response.

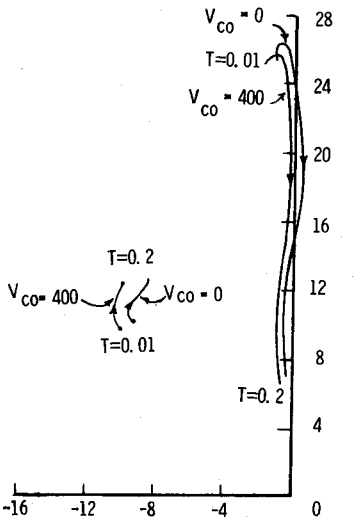

Fig. 5 Equivalent s-plane pole location for suboptimal controller.

A root square locus of the optimal closed-loop poles using Eq. (24) and the rigid-body model are shown on Fig. 2 for various crossover velocities. As expected, the closed-loop damping ratio varies directly with V_{co}. It is interesting to note that choosing V_{co} in the range of 200-400 ft/s results in the optimal system having a closed-loop damping ratio of about 0.7, while retaining reasonable closed-loop bandwidth. For further analysis, four different crossover velocities of 0, 200, 400, and 600 ft/s were chosen with appropriate values of ρ so that the closed-loop damping ratio equals 0.7.

Response to External Disturbance

These systems were evaluated by determining the steady-state covariances of state and control in response to a white noise gust input. The white noise assumption was considered appropriate for comparison purposes of the different models, although for more realistic simulations of aircraft responses, alternate gust models are available.[8] The responses were calculated and compared using the control block diagram as shown in Fig. 3.

In general, the response to the external disturbance increases for all cases as the sampling interval increases, as shown in Fig. 4. For the suboptimal control based on rigid-body assumptions, the mean square responses do, in fact, improve at very low sample rates (less than about 5-8 samples per second), but this effect is of little practical significance.

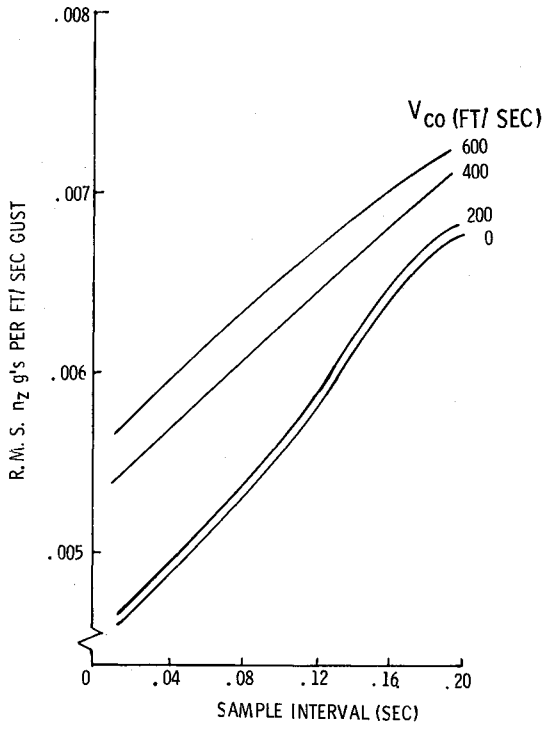

Fig. 6 Load factor response of optimal controller.

The peak in the suboptimal curves of Fig. 4 appears to result from the commensurability of the closed-loop structural frequency and the Nyquist frequency (half the sampling frequency) at these low rates. The performance of the suboptimal system deteriorates at low sample rates due to the migration of the equivalent s-plane poles of the structural mode, as shown in Fig. 5. It is seen that for the assumed sensor locations, the controls designed using the rigid-body approximation may result in an unstable system. Increasing the crossover velocity in a C^*-type performance index has the advantage of alleviating this problem by moving these poles further into the left half of the s-plane. This reduces the response peaks at low sample rates and aids in stabilization of the system. For the optimal system, the expected value of load factor (Fig. 6) will, in fact, increase with an increase in crossover velocity for a fixed sample rate, while the mean square response in pitch rate (Fig. 4) decreases. This is due to the fact that an increase in V_{co} increases the relative weight on the pitch rate term in the performance index. For the case of optimal feedback, the average increase in normalized load factor response was about 40% and the increase in response of angle of attack was about 60% for the range of sampling time considered.

In general, there is very little improvement in response by using an optimal feedback law over the suboptimal control law for sampling rates higher than about 10 samples per second. It is seen in Fig. 7, for example, that the rms load factor of the suboptimal design may be lower than that obtained using the exact control model. Inserting the notch filter in the control loop, using the previously mentioned method of discretization, always increased the response as seen in the figure. The reason for the large increase in response due to the addition of the notch filter is not yet fully understood and is under further investigation.

Conclusions

For the cases considered, the suboptimal controller, designed using only rigid-body information, is adequate for low or moderate sample rates as there is no significant improvement in response by using an optimal control law. At slow sample rates, less than about 10 samples per second, the optimal feedback law is superior to the suboptimal control, which can sometimes yield an unstable closed system. The conclusion is that the rigid body feedback laws are adequate to insure a good system response for moderate sampling rates. However, an accurate control model can maintain good mean-square response characteristics for very low sampling rates, thereby freeing some of the computational burden from the flight control computer. Whether these low rates are adequate for other control tasks is an additional question which needs to be addressed.

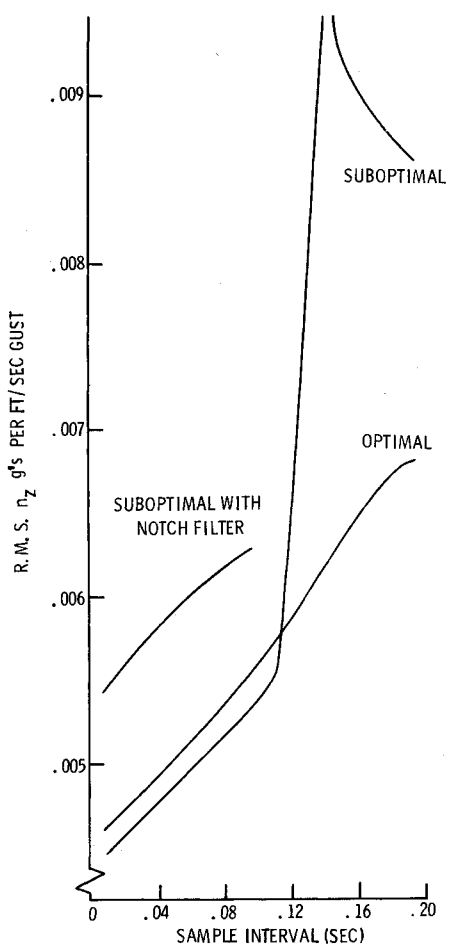

Fig. 7 Comparison of load factor response for $V_{co} = 0$ ft/s.

References

[1] Berman, H. and Gran, R., "An Organized Approach to the Digital Autopilot Design Problem," AIAA Paper 73-848, AIAA Guidance and Control Conference, Key Biscayne, Fla., Aug. 1973.

[2] Katz, P. and Powell, J. D., "Selection of Sampling Rates for Digital Control of Aircraft," SUDDAR Rept. 486, Stanford University, Stanford, Calif., Sept. 1974.

[3] Melzer, S. M. and Kuo, B. C., "Sampling Period Sensitivity of the Optimal Sampled Data Linear Regulator," *Automatica*, Vol. 7, 1971, pp. 367-370.

[4] Levis, A. H., Athans, M., and Schlueter, R.A., "On the Behavior of Optimal Linear Sampled Data Regulators," *International Journal of Control*, Vol. 13, Feb. 1971, pp. 343-361.

[5] Bryson, A. E. and Ho, Y. C., *Applied Optimal Control*, Ginn-Blaisdell, Waltham, Mass., 1969.

[6] Slater, G. L., "A Unified Approach to Digital Flight Control Algorithms," AIAA Paper 74-884, AIAA Mechanics and Control of Flight Conference, Anaheim, Calif., Aug. 1974.

[7] Hartman, G. L., Hauge, J.A., and Hendrick, R.C., "F-8C Digital CCV Flight Control Laws," NASA CR-2629, Feb. 1976.

[8] Chalk, C. R., Neal, T.P., Harris, T.M., Pritchard, F.E., and Woodcock, R.J., "Background Information and User Guide for MIL-F-8785B (ASG), Military Specification-Flying Qualities of Piloted Airplanes," Air Force Flight Dynamics Lab. Tech. Rept. AFFDL-TR-69-72, Aug. 1969.